Supplementary Information

ICG-Loaded and ^{125}I-Labeled Theranostic Nanosystem for Multimodality Imaging-Guided Phototherapy of Breast Cancer

Dianyu Wang,[a,#] Jianlan Yue,[b,c,#] Qiannan Cao,[a,#] Jinjian Liu,[a] Lijun Yang,[a,*] Wen Shen,[d,*] Wenxue Zhang,[e,*] and Jianfeng Liu[a,*]

[a] Key Laboratory of Radiopharmacokinetics for Innovative Drugs, Chinese Academy of Medical Sciences, and Institute of Radiation Medicine, Chinese Academy of Medical Sciences & Peking Union Medical College, Tianjin 300192, P. R. China.

[b] Department of Radiology, First Central Clinical College, Tianjin Medical University, Tianjin 300192, P. R. China.

[c] Department of Nuclear Medicine, Characteristic Medical Center of Chinese People's Armed Police Forces, Tianjin 300162, P. R. China.

[d] Department of Radiology, Tianjin First Central Hospital, School of Medicine, Nankai University, Tianjin 300192, P. R. China.

[e] Radiation Oncology Department, Tianjin Medical University General Hospital, Tianjin 300052, P. R. China.

[#] These authors contributed equally to this work.

* Corresponding authors

Prof. Lijun Yang, E-mail address: yanglijun@irm-cams.ac.cn

Prof. Wen Shen, E-mail address: shenwen66happy@126.com

Prof. Wenxue Zhang, E-mail address: wenxuezhang@tmu.edu.cn

Prof. Jianfeng Liu, E-mail address: liujianfeng@irm-cams.ac.cn

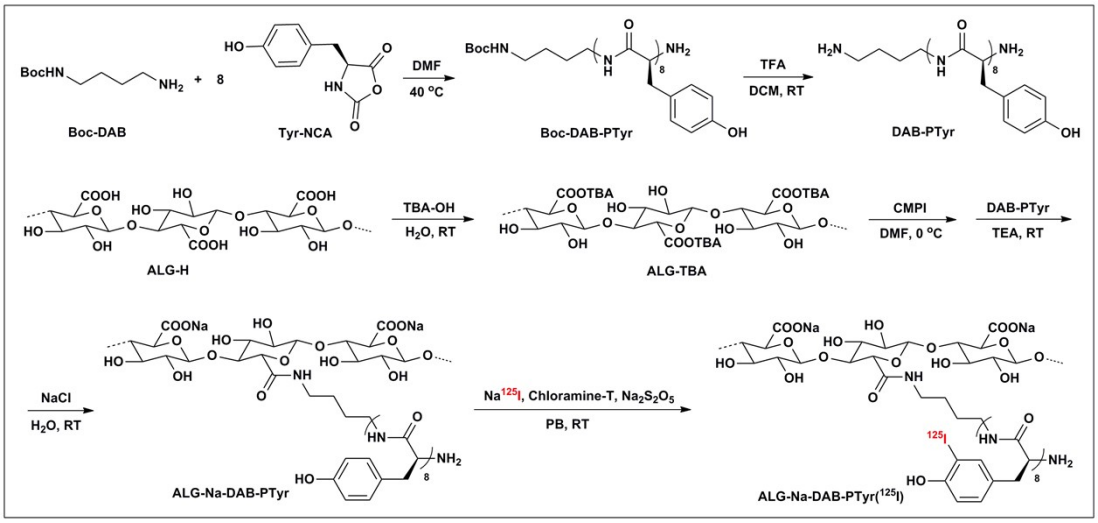

Fig. S1 The synthesis route for ALG-Na-DAB-PTyr(^{125}I).

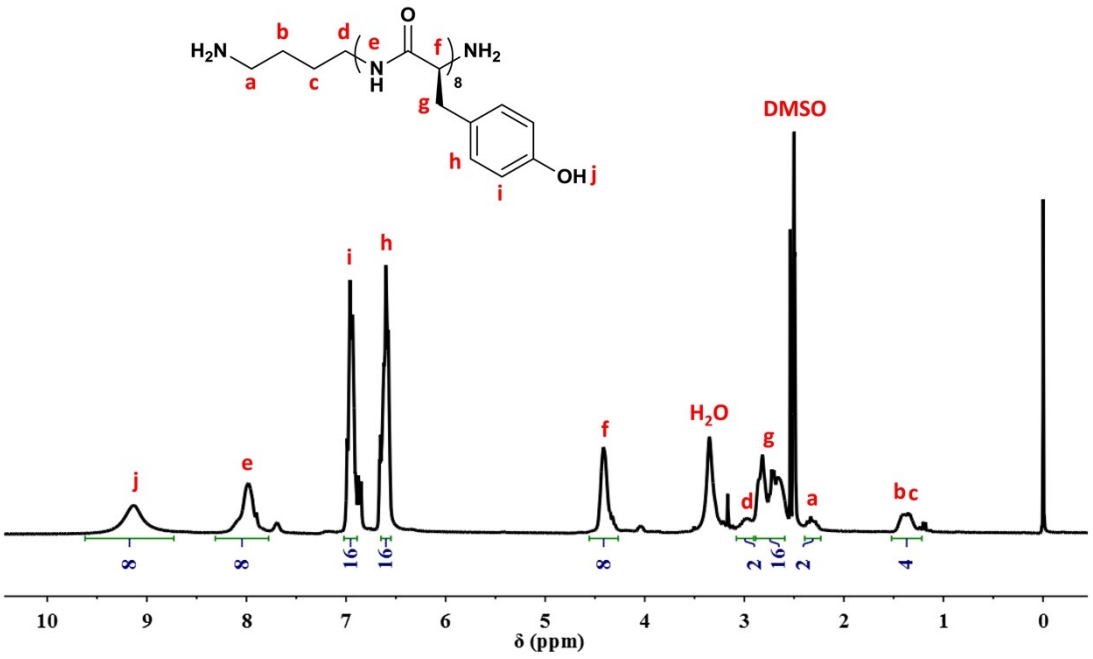

Fig. S2 ^{1}H NMR spectrum of DAB-PTyr in DMSO-d_6.

Element	C%	H%	N%
Content	34.31	5.52	1.13

Fig. S3 The elemental analysis of ALG-Na-DAB-PTyr.

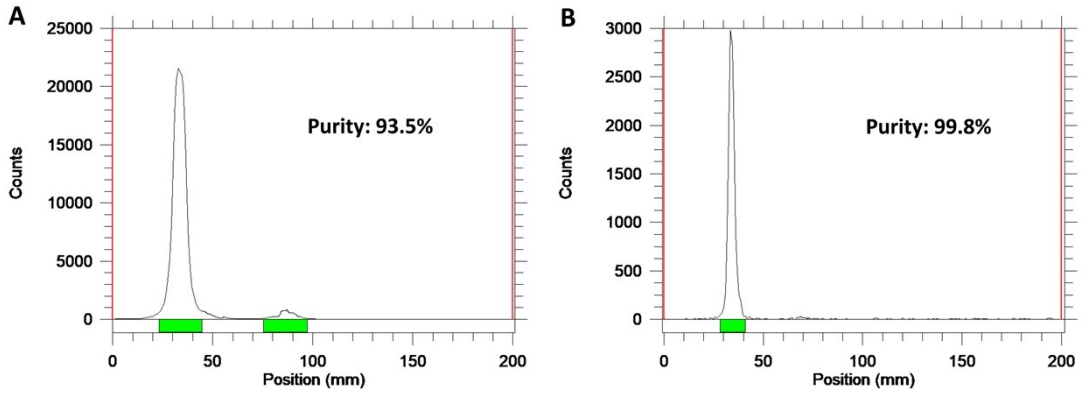

Fig. S4 The radiolabeling rate (A) and the radiochemical purity (B) of ALG-Na-DAB-PTyr(^{125}I) determined by a radioactive TLC scanner.

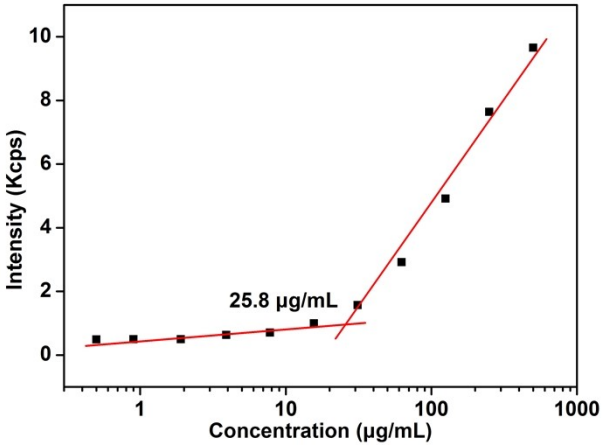

Fig. S5 The CMC of ADY(^{125}I) NPs determined by using Nile Red as the fluorescence probe.

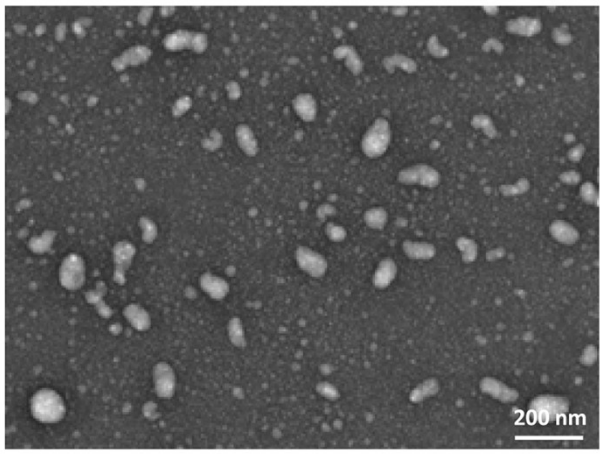

Fig. S6 The representative TEM image of ADY(^{125}I) NPs.

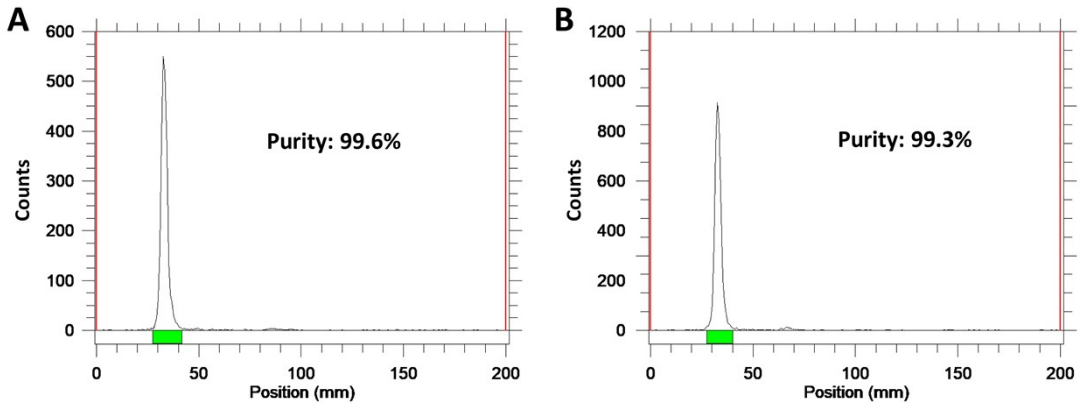

Fig. S7 The radiochemical purity of ICG@ADY(^{125}I) NPs before (A) and after (B) 48 h of incubation with mouse plasma.

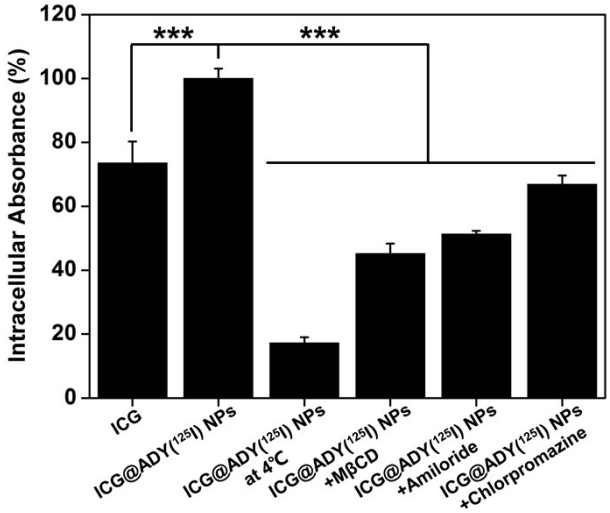

Fig. S8 Quantitative analysis of ICG in 4T1 cells after the treatment with ICG or ICG@ADY(^{125}I) NPs with or without various inhibitors using a UV-visible spectrophotometer. The data are presented as the mean ± SD (n = 3). *** stands for $P < 0.001$.

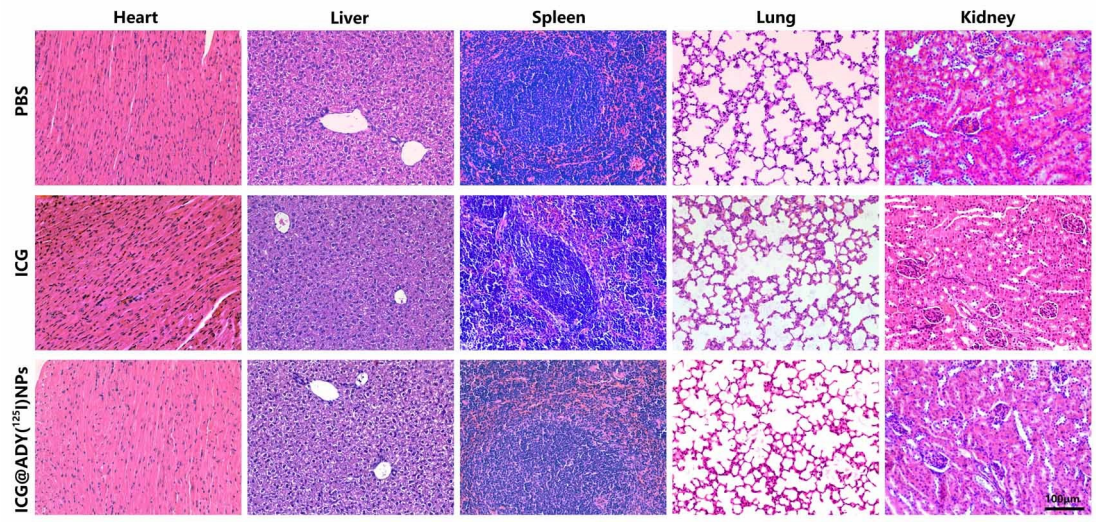

Fig. S9 H&E stained tissue sections from the heart, liver, spleen, lung, and kidney of the healthy BALB/c mice one week after the two successive days of administration of PBS, ICG, or ICG@ADY(^{125}I) NPs.

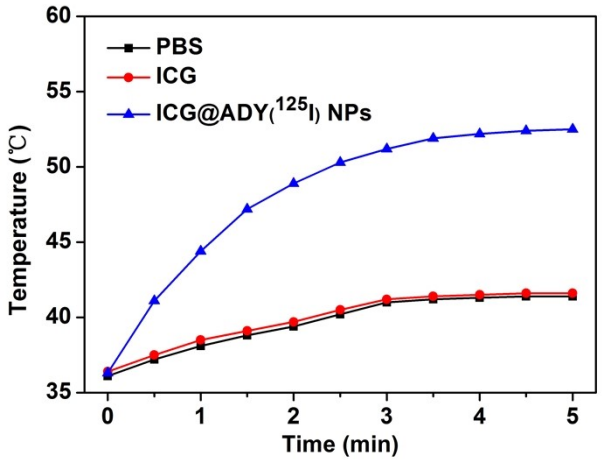

Fig. S10 The intratumoral temperatures of the 4T1 tumor-bearing mice during an 808 nm laser (1 W/cm^2) irradiation 24 h after the intravenous administration of PBS, ICG, or ICG@ADY(^{125}I) NPs.

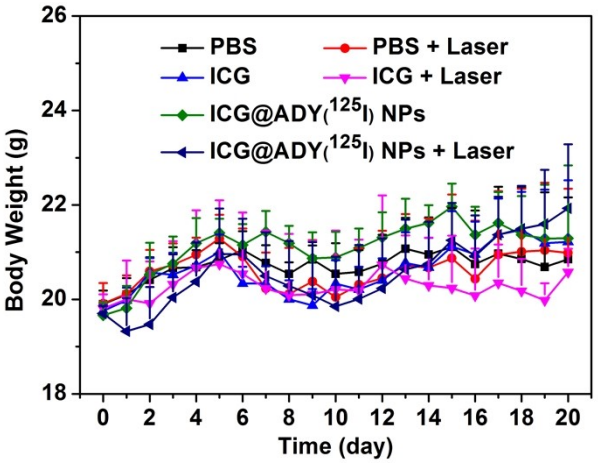

Fig. S11 Body weight changes in the tumor-bearing mice with various treatments. The data are presented as the mean ± SD (n = 5).

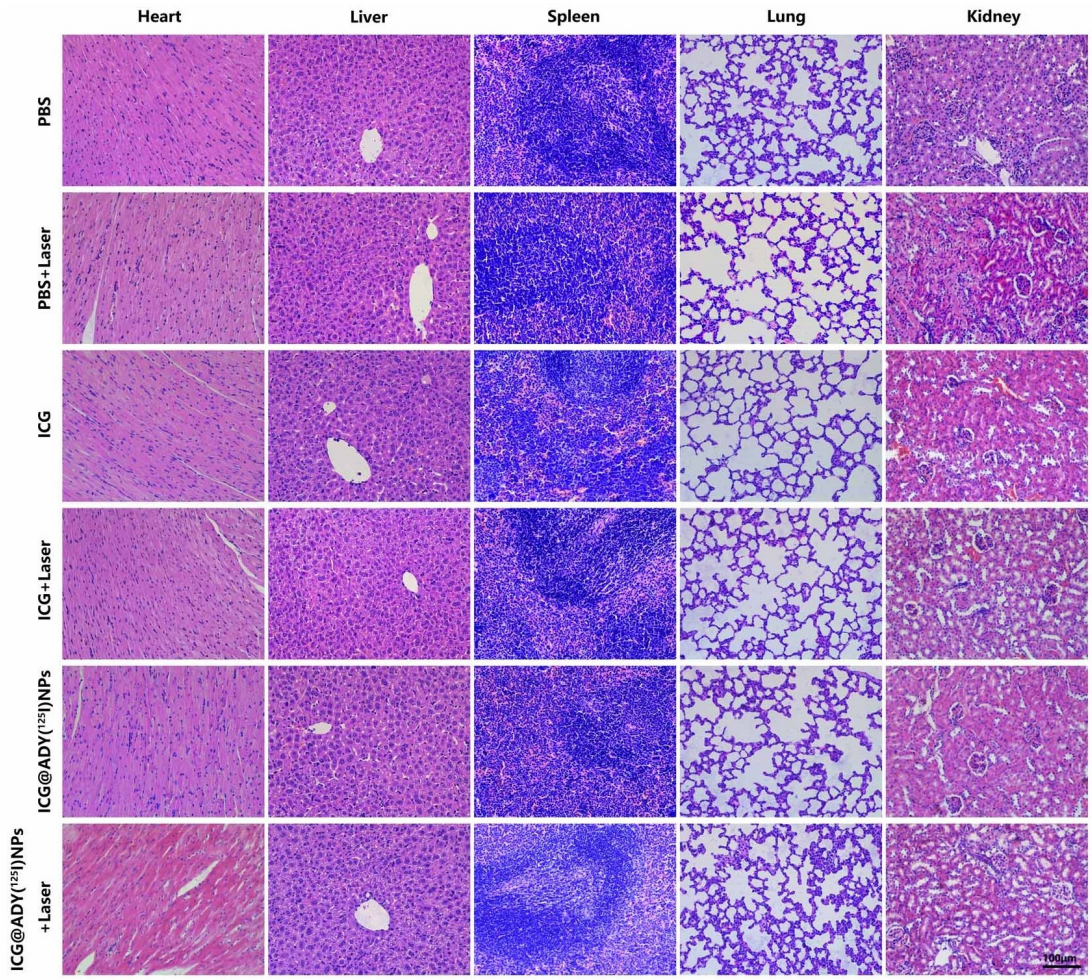

Fig. S12 H&E-stained tissue sections from the heart, liver, spleen, lung, and kidney of the 4T1 tumor-bearing nude mice on the 20th day after PTT/PDT.